Investigation of a Two-stage Boost converter using the Neutral Point of a Motor

Jun-ichi Itoh*, Daisuke Ikarashi*

* Nagaoka University of Technology, 1603-1 Kamitomioka-cho Nagaoka City, Niigata 940-2188, Japan

***Abstract*--Control strategy and loss evaluation is discussed for a proposed DC/AC two-stage boost converter using the neutral point of a motor. The proposed converter consists of a small boost chopper and a three-phase inverter, which has a boost up function from the use of the leakage inductance of a motor, instead of a boost-up reactor, for DC to AC conversion. A six-step operation strategy is proposed for the circuit. When the inverter part outputs a square waveform of 180°, the input current has a distortion because the neutral point voltage of the motor fluctuates at a frequency three times of the output frequency. The input current is also shown distorted due to the neutral point voltage fluctuation. Feed forward compensation is proposed to reduce the input current fluctuation. In addition, the DC current in the proposed circuit is imposed into the phase current of the motor. Loss evaluation is therefore implemented to investigate the influence of the imposed DC current on the experimental results. Also, finite element method (FEM) was used to analyze the motor loss for a 1.5 kW interior permanent-magnet (IPM) motor.**

***Index Terms*—DC-DC power conversion, DC-AC power conversion, Pulse width modulated inverters, Permanent magnet motors, Motor drives, Inductance**

I. INTRODUCTION

Recently, motor drive technologies that employ batteries are required in many applications, such as electric vehicles and railway trains [1-3]. In a motor drive system, high voltage is generally preferable than high current because a higher motor current degrades the motor efficiency. However, a high volume of battery bank is required to provide high voltage in a motor drive system. Therefore, a boost converter is usually connected with the batteries before connecting to the inverter stage. The boost converter can increase the DC voltage at the same time reduce the battery volume.

Figure 1 shows a conventional DC/AC power converter which is composed of batteries, a boost converter and a three-phase inverter. Battery voltage is increased by the boost converter when the inverter outputs high voltage to the motor. However, the boost converter requires a large boost-up reactor, which is costly and bulky. In addition, high switching frequency is applied to reduce the volume of the boost-up reactor; however, the switching loss is increased as a trade-off. One solution to reduce the switching losses under high frequency is to use resonance converters [4-8]; however, this approach will increase the number of components use in the boost converter.

In order to solve this problem, the authors have proposed a reactor free boost converter that uses the leakage inductance of a motor instead of a boost-up reactor [9-13]. Figure 2 shows the DC/AC conversion reactor free boost converter [10-11]. In the proposed converter, the neutral point of a motor is directly connected to batteries, so that the inverter output voltage can be increased without increasing the number of components.

However, the proposed converter has three practical problems:

(i) *Limitation of the inverter output voltage*

Figure 3 shows the controllable range of the inverter output voltage for the DC/AC conversion reactor free boost converter. The maximum value of the inverter output phase voltage is limited to 0.5 when the boost-up ratio is two. The higher the boost-up ratio the lower is the output voltage can be achieved, because the modulation index of the inverter is saturated by a zero-phase component.

(ii) *Ripple current caused by the six-step operation*

One of the control methods for a motor drive is six-step operation. Implementation of six-step operation in the inverter can increase the voltage utilization and achieve higher inverter efficiency than pulse-width modulation (PWM) operation, because the switching frequency for six-step operation is lower than that for PWM operation, particularly in the high frequency application, the PWM operation generates higher losses in the inverter than the motor. In Fig. 2, when six-step operation is applied to the inverter control, the neutral point voltage of the motor will fluctuate at a frequency which is three times of the output frequency. The battery is connected to the neutral point of the motor; therefore, the input current will contain a large ripple due to the fluctuation of the neutral point voltage of the motor.

(iii) *Increase of the motor loss*

In the reactor free boost converter, a DC current is imposed into the phase current of the motor, which results the copper loss of the motor will increase. Under ideal conditions, the zero-phase current in the motor does not generate motor torque and iron loss, because the zero-phase flux is denied with each other. However, the magnetic flux density may be increased by the zero-phase current, although the influence of the zero-phase current in the motor has not yet been clarified.

This paper discusses a two-stage boost converter using the neutral point of a motor to solve problems (i) and (ii). The proposed circuit consists of batteries, a three-phase inverter that connects to the neutral point of a motor, and a small boost converter. The proposed circuit can reduce the terminal voltage of the boost-up reactor, and as a result, the size of the boost-up reactor and switching losses in the boost converter are reduced. In addition, the current fluctuation at the neutral point of the motor resulting from six-step operation is compensated by a current regulator and feed forward control in a small stage boost converter. The validity of the proposed converter and its control strategy are confirmed by experimental results. Furthermore, loss evaluation of the proposed circuit is analyzed and compared with that to a conventional circuit. Finally, in consideration of the motor loss and torque ripple, the influence of (iii) is analyzed using a 2D finite element method (FEM) on a 1.5 kW interior permanent-magnet (IPM) motor.

II. CIRCUIT TOPOLOGY

A. Circuit configuration

Figure 4 shows the proposed circuit configuration, which is composed of batteries, a three-phase inverter and a first stage boost converter that connects to the neutral point of a motor. The inverter in the proposed circuit has a boost-up function when the motor leakage inductance is utilized. However, a DC current is imposed to the phase current of the motor in the proposed circuit.

The proposed circuit can reduce the volume of the boost-up reactor and switching losses in the first stage boost converter. When a sinusoidal wave triangle carrier comparison method is used to generate PWM pulses, the neutral point voltage of the motor is the same as that of the DC link part, i.e., half of the DC link voltage E_{dc1}. Therefore, the voltage rating of the boost-up reactor and switching device in the first stage boost converter is reduced to half that of the DC link voltage. It should be noted that the capacitor C_2 connected to the neutral point of the motor is 100 times smaller than the DC link capacitor C_1 of the inverter; therefore, C_2 is not bulky.

The applied voltage of the boost-up reactor is assumed to be constant during a switching cycle. Therefore, the relationship between the inductance of boost-up reactor L and the input current ripple ΔI_{in} can be expressed as

$$\Delta i_{in} = \frac{1}{L}\int_0^{d/f_{sw}} v_L dt = \frac{v_L d}{L f_{sw}} \quad \text{.....(1),}$$

where d is the duty ratio, f_{sw} is the switching frequency, and v_{L} is the applied voltage of the reactor.

When the input current ripple ΔI_{in} is designed, the required inductance of the boost-up reactor L is derived from (1).

Figure 5 shows the relationship between the boost-up ratio and the inductance reduction ratio in the proposed circuit. When the boost-up ratio is three, the proposed circuit can reduce the inductance of the boost-up reactor by half compared to the conventional circuit. Therefore, the proposed circuit can employ boost-up reactor of

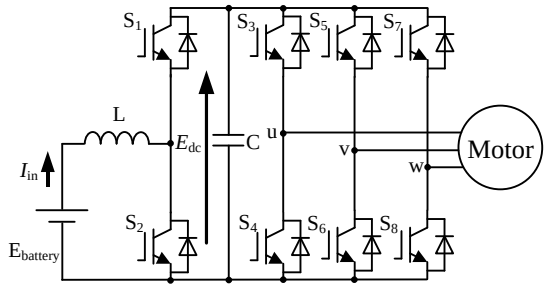

Fig. 1. Conventional circuit diagram.

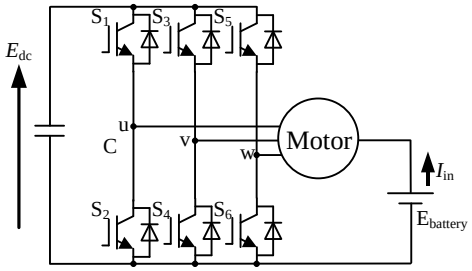

Fig. 2. Reactor free boost converter for DC/AC conversion.

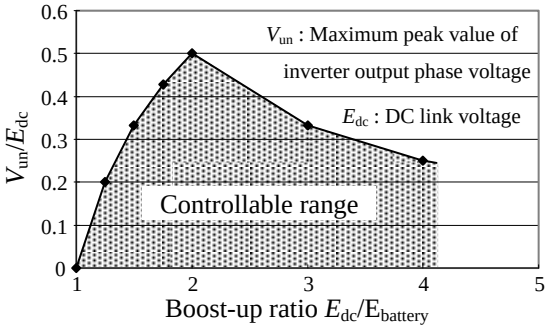

Fig. 3. Controllable range of the converter in Fig. 2.

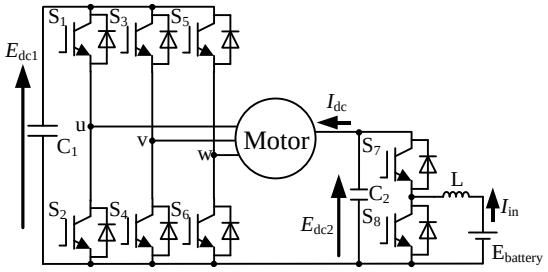

Fig. 4. Proposed circuit diagram.

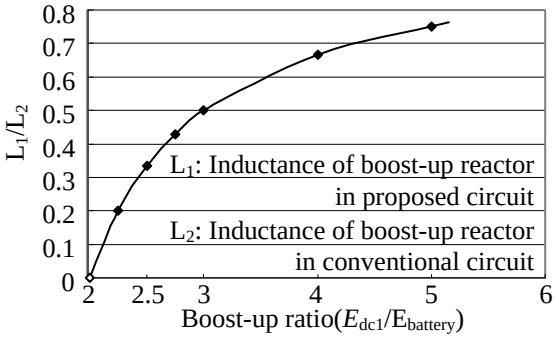

Fig. 5. Relationship between the boost-up ratio and the reduction ratio of inductance in the proposed circuit.

reduced size.

B. Positive phase sequence equivalent circuit

Figure 6 shows a positive-phase sequence equivalent circuit for the proposed circuit. The proposed circuit can be divided into positive and zero sequence components. The boost converter does not appear in the positive-phase sequence equivalent circuit, due to the connection to the neutral point of the motor. Consequently, the positive-phase sequence equivalent circuit is similar to a conventional three-phase inverter. During PWM control, when a sinusoidal modulation based on triangle carrier comparison is used to generate PWM pulses, the fundamental voltage of the output is given by

$$V_{out} = \frac{\sqrt{3}}{2\sqrt{2}} E_{dc} \cdot a \quad \text{.....(2),}$$

where V_{out} is the output line voltage, E_{dc} is the DC link voltage, and a is the modulation index.

In the proposed circuit, a six-step operation is applied to the three-phase inverter in order to reduce the switching loss of the inverter compared with that for a PWM inverter. During the six-step operation, the switching frequency agrees with the output frequency. The output line voltage becomes a 120° square waveform, and the fundamental voltage of the output is then given by

$$V_{out} = \frac{\sqrt{6}}{\pi} E_{dc} \quad \text{.....(3).}$$

C. Zero phase sequence equivalent circuit

Figure 7 shows the zero-phase sequence equivalent circuit. The back electromotive force (EMF) does not appear in the zero-phase sequence equivalent circuit, but only the leakage inductance exists. In the zero-phase sequence, the inverter legs could be considered as a single leg. The output voltage of the single leg is the same as the neutral point voltage of the motor. A two-stage boost up operation is achieved using two choppers constructed by switches S_1 and S_2, and switches S_3 and S_4. However, the leakage inductance of the motor decreases to 1/3, because the leakage inductance of the motor is connected in parallel in the zero-phase sequence equivalent circuit.

The neutral point voltage of the motor is given by

$$E_{dc2} = \frac{1}{3}(v_u + v_v + v_w) + \frac{1}{2} E_{dc1} \quad \text{.....(4),}$$

where E_{dc2} is the neutral point voltage of the motor, v_u, v_v and v_w are the motor phase voltages and E_{dc1} is the DC link voltage.

Therefore, the neutral point voltage of the motor can be controlled by the zero-phase voltage command. In particular, the average neutral point voltage of the motor for one switching period is zero when a symmetrical three-phase sinusoidal waveform is used as the modulation signal. Therefore, the neutral point voltage of the motor is equal to double the DC link voltage. Furthermore, the sum of the maximum inverter output voltage command and the zero-phase voltage command is limited by the neutral point voltage of the motor. If the battery is directly connected to the neutral point of the motor, then the maximum phase voltage of the motor is constrained by the battery voltage, as shown in Fig. 3. However, in the proposed circuit, the maximum phase voltage is not constrained by the battery voltage, because the neutral point voltage of the motor is controlled by the boost converter.

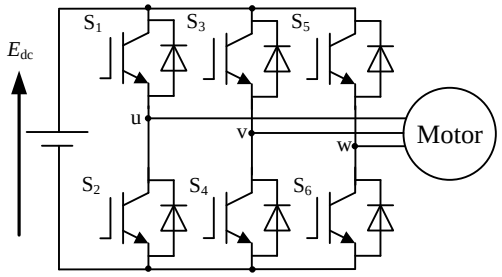

Fig. 6. Positive phase sequence equivalent circuit for the proposed circuit.

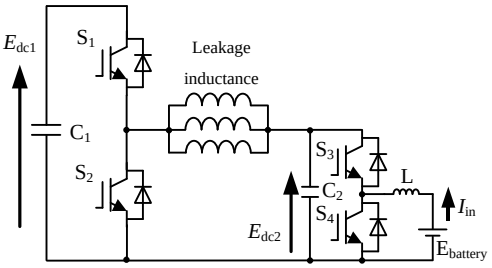

Fig. 7. Zero phase sequence equivalent circuit.

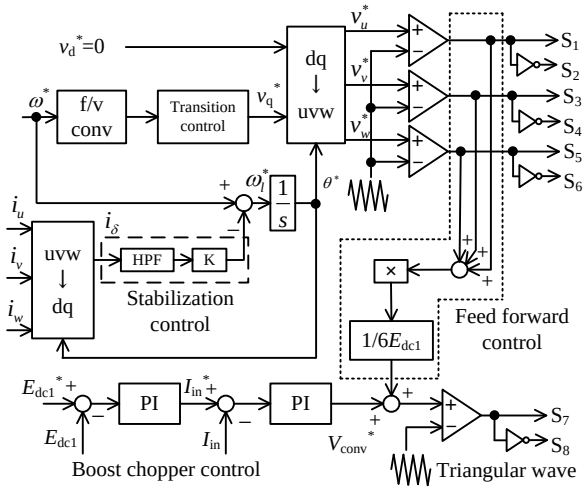

Fig. 8. Control block diagram.

III. Control Strategy

A. Output voltage control method

Figure 8 shows the block diagram for the proposed circuit. Control of the motor current in the proposed circuit is the same as that for a conventional three-phase inverter, because the positive-phase sequence equivalent circuit is exactly the same as that for a conventional three-phase inverter. A stabilization control is applied to achieve *V/f* control for a permanent magnetic (PM) motor [14]. The stabilization control consists of a high-pass filter and feedback from the q-axis current. In addition, the PWM control is slowly changed to six-step operation

via trapezoidal pulse modulation [15]. The transition control shown in Fig. 8 is compensation that is proportional to the amplitude of the output voltage command, because the output voltage increases nonlinearly in the trapezoidal pulse area.

The transition control shown in Fig. 8 controls the output voltage proportional to the output frequency under a V/f constant condition. It is based on the non-linear control of the fundamental frequency which proportionally compensates the amplitude of the output voltage command. During the transition period, the amplitude of v_q will be extended by gain according to the modulation index and frequency. The transition control will automatically activated when the modulation index of inverter (a) is larger than 1.0.

B. Battery current compensation control

When the six-step operation is applied to the inverter control in the proposed circuit, the input current is distorted at three times the output frequency. The reason for this is that the neutral point voltage of the motor has a fluctuation of $\pm 1/6E_{dc1}$ with three times the inverter output frequency in the six-step operation. In order to compensate the voltage fluctuation, feed forward control is applied to a current regulator in the first stage boost converter. The voltage fluctuation is estimated by the DC link voltage and the pulse pattern of the inverter [15].

As shown in Figure 8, the first stage boost converter uses two PI regulators to regulate the DC link voltage (E_{dc1}) and input current (I_{in}). To compensate the neutral point fluctuation, the sum of the three output phase voltage which is 1/6 Edc is first normalized and then added into the output of the PI controller. After normalization, the feed forward signal becomes an inversed waveform of the PI regulator output signal. Then, the feed forward waveform balances the output signal of the PI controller before comparing with the triangular carrier.

IV. EXPERIMENTAL RESULTS

A. Experimental results with PWM control

Table 1 shows the experimental parameters for the PM motor and the battery voltage. Figure 9 shows the experimental results during PWM control. During this experiment, the output torque was controlled to 100%. The E_{dc1} is 286 V and E_{dc2} is 143 V. From Fig. 9, it is confirmed that the neutral point voltage of the motor is increased to double that of the DC link voltage by the inverter side boost-up function that utilizes the motor leakage inductance. Furthermore, the motor current has DC components, because the motor current is added to the zero-phase current. However, sinusoidal motor current waveform and sinusoidal line voltage of the motor are obtained. It should be noted that the output line voltage V_{uv} is observed using a low-pass filter (LPF) with a 1.5 kHz cut-off frequency to observe the low frequency component distortion.

B. Experimental results with Six-step operation

TABLE I
EXPERIMENTAL PARAMETERS

Battery voltage $V_{battery}$	70[V]
Output frequency	90[Hz]
PM motor rated output	750[W]
Rated voltage	175[V]
Rated current	3.3[A]
Boost chopper reactor L	1.7[mH]
Zero phase inductance	1.9[mH]
Capacitor C_1	1100[mF]
Capacitor C_2	5.0[mF]

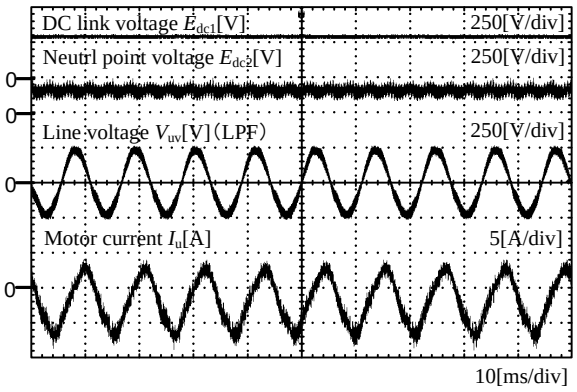

Fig. 9. Experimental results with PWM control.

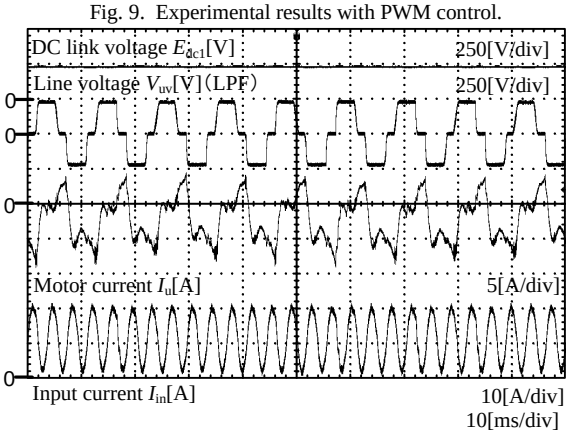

(a) Experimental results without feed forward compensation.

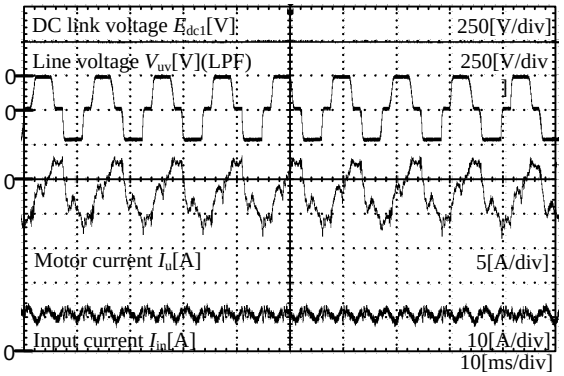

(b) Experimental results with feed forward compensation.
Fig. 10. Six-step operation experimental results.

Figure 10 shows the experimental results during six-step operation. In this experiment, the output torque is controlled to 75%. Note that the rated torque is reduced to 75% due to the reason current ripple will damage the motor when the feed forward is not applied. In Fig. 10(a),

a fluctuation occurs in the input current, because the neutral point voltage of the motor has fluctuation. Figure 10(b) shows that the ripple in the input current is suppressed by the proposed control.

Figure 11 shows results for harmonic analysis of the input current. In Fig. 11(a), the input current is confirmed to contain the third harmonic component of the output frequency. For Fig. 11(b), feed forward compensation is applied and the input current ripple is suppressed. In comparison with Fig. 11(a), the third harmonic component of the output frequency in the input current is suppressed and is 1/8 of its original value.

C. Acceleration characteristic

Figure 12 shows the acceleration characteristics from PWM operation to six-step operation. PWM control is gradually changed into the six-step operation, which can be confirmed by the u-v line voltage. The pulse mode moves entirely from PWM into six-step operation without appearance of a rush current.

In this result, IPM is applied with V/f constant control, during the PWM control the modulation index of the inverter is lower than 1.0 and starting from 1Hz to 71Hz. The transition control starts as the output frequency increases from 72Hz to 89 Hz, which is proportionally to the output voltage command where the modulation index starts from 1.0. Then the six-step is completed at frequency 90 Hz, where the modulation index of the inverter becomes 1.27.

Note that this result was conducted at no load condition, where the motor current is dominated by d-axis current (reactive current). During the PWM control, the E_{dc1} is 224V and E_{dc2} is 112V, which has a lower boost-up ratio than the case of Fig. 9.

D. Torque Impact characteristic

Figure 13 shows the torque impact characteristics. The output frequency is 90 Hz, and the step increase of torque is 100%. The results confirm stability to the load step. Furthermore, the DC link voltage E_{dc1} vibration is suppressed by the voltage regulator.

V. Loss Analysis & Efficiency

Figure 14 shows a converter loss comparison between the conventional circuit shown in Fig. 1 and the

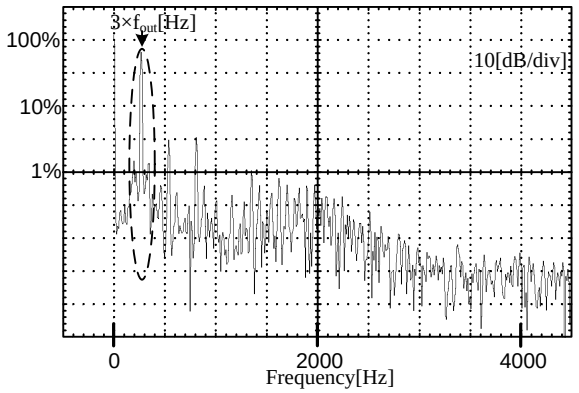

(a) Harmonics analysis without feed forward compensation.

(b)

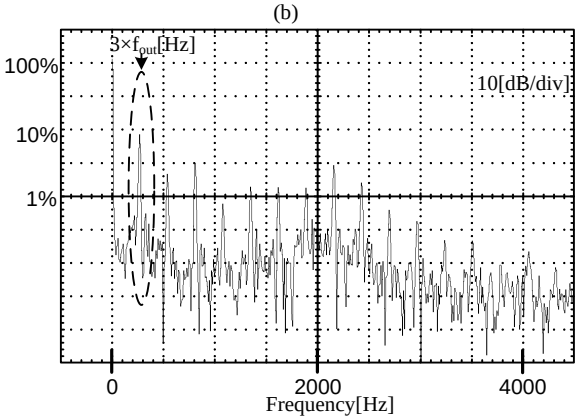

(b) Harmonics analysis with feed forward compensation.

Fig. 11. Input current harmonics analysis.

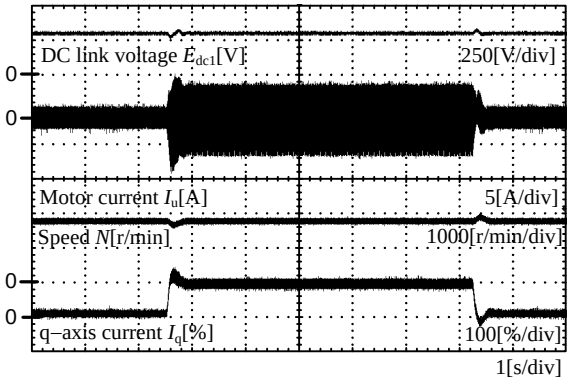

Fig. 13. Torque impact characteristics.

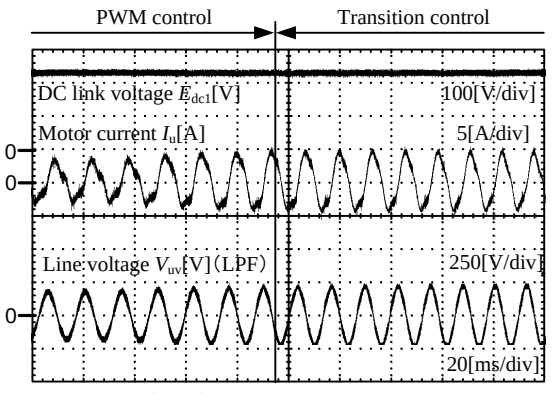

(a) Operation waveform from PWM control to transition control.

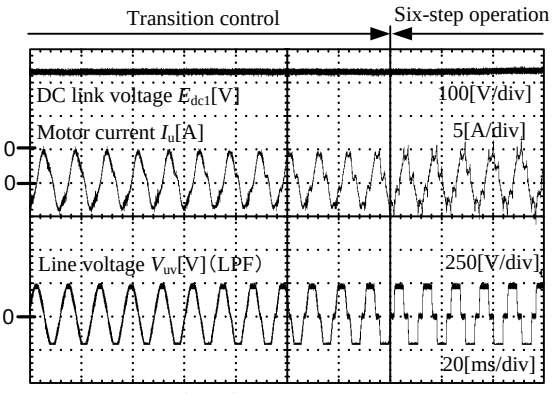

(b) Operation waveform from transition control to six-step operation.

Fig. 12. Acceleration characteristics.

proposed two-stage circuit based on the experimental results during a PWM control. The inverter loss in the proposed circuit is measured with a three-phase four-wire system. The proposed circuit is confirmed to reduce converter loss by 10% compared with that for the conventional circuit at the rated operation, because the proposed circuit can decrease the boost converter loss.

Figure 15 shows the total loss comparison of the proposed system with the conventional system. The losses of the boost-up reactor are included in the boost converter loss. The efficiency of the boost converter in the proposed circuit is 1.7 % higher. This reasons that the terminal voltage of the switching device in the boost converter decreases to less than 1/2 it voltage value for the conventional circuit. Therefore, the switching loss in the boost converter is decreased by half. Similarly, the half voltage rating switching device can be used in the first stage boost converter of the proposed circuit. Therefore, if the lower voltage rating switching device is used in the first stage boost converter, the loss can be reduced. Furthermore, the copper loss of the boost-up reactor can be decreased and the proposed circuit can reduce the size of the boost-up reactor due to the low voltage terminal. The second stage boost converter however needs to use a higher voltage rating devices because the DC link voltage is similar to the conventional boost converter.

However, the inverter losses and the motor losses are increased because the DC current is imposed into the phase current of the motor in the proposed circuit.

VI. Magnetic field analysis results

In order to consider the behavior of the imposed DC current in the motor, a 2D finite element method (FEM) is demonstrated by simulating a 1.5 kW IPM motor [16]. It should be noted that the experimental results uses 750 W IPM motor due to limitation on the experimental setup. Table 2 shows the IPM motor parameters. Two conditions are considered. The first is that the motor phase current is assumed to be a sinusoidal rated current without a DC current. The second condition is the sinusoidal waveform is added with a DC current, where the DC current is -3.14 A per single phase.

Figures 16(a) and (b) show the magnetic flux density distributions of a 1.5 kW IPM motor, in (a) where the motor current is a sinusoidal waveform, and in (b) the DC current is included in the sinusoidal waveform, respectively. The magnetic flux density distribution is almost the same under both conditions. Therefore, it can be confirmed that the increase of iron loss caused by the zero-phase current is very low.

Figure 17 shows a comparison of flux density between (a) and (b) taken near the stator slot named “observation point”. The result shows that the flux density of the proposed circuit is increased by approximately 10%, which is affected by the DC component.

Figure 18 shows a comparison of the motor torque waveforms with and without DC. In this 2-D FEM simulation, the rotor skew is not considered. Therefore, the absolute value of the torque ripple should not be

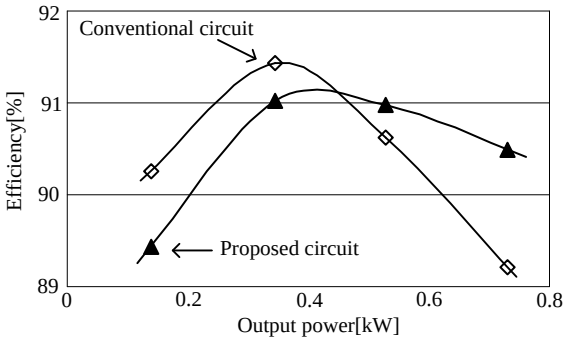

Fig.14. The converter efficiency comparison of the conventional circuit with the proposed circuit.

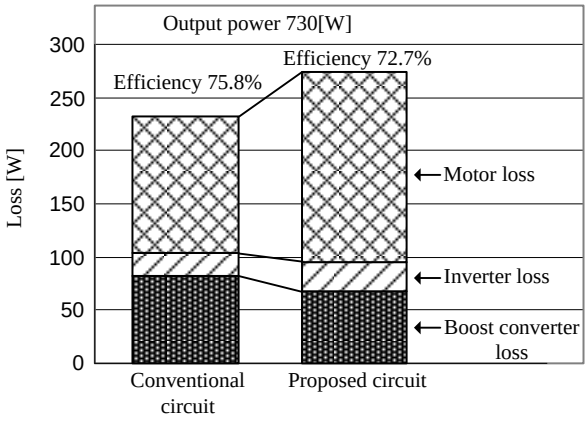

Fig. 15. Total loss comparison between the proposed system and a conventional system.

TABLE II
IPM motor Parameters

Motor power	1.5 [kW]
Rated voltage	180 [V/phase]
Rated current	6.1 [A]
Rated speed	1800 [rpm]
Number of poles	6 poles
Number of stator slots	36 slots
Stator outer diameter	130 [mm]
Stator inner diameter	83 [mm]
Winding configuration	138turn, series per phase
Rotor outer diameter	82.2 [mm]
Rotor shaft diameter	30 [mm]

discussed. The point of this simulation is that the torque ripple is increased by 10% when the DC current is added to the output current. This means that the torque ripple is affected by DC current, which contains the third harmonic component of EMF and the space harmonic components. It should be noted that the torque ripple resulting from the third harmonic component can be compensated by feed forward control.

Figure 19 shows a comparison of the total loss distribution in the simulation. Table II shows the motor parameters. For the conventional circuit, the E_{dc} is 294V and for the proposed circuit, the E_{dc1} is 294V and E_{dc2} is 147V. Similarly to Figure 15, the inverter loss of the proposed circuit increases because the I_{dc} is added into the inverter current, which is caused by boost-up operation of the second-stage boost converter.

On the other hand, the loss of first-stage boost converter reduces because the E_{dc2} voltage is

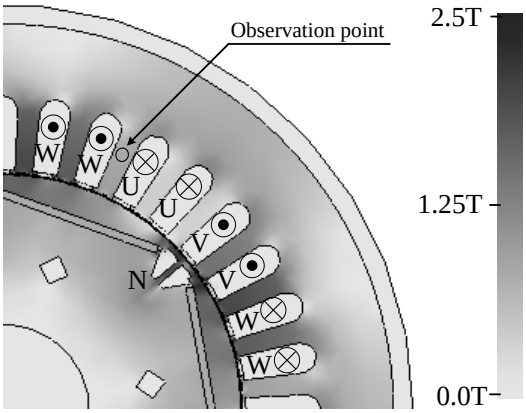

(a) Without DC current.

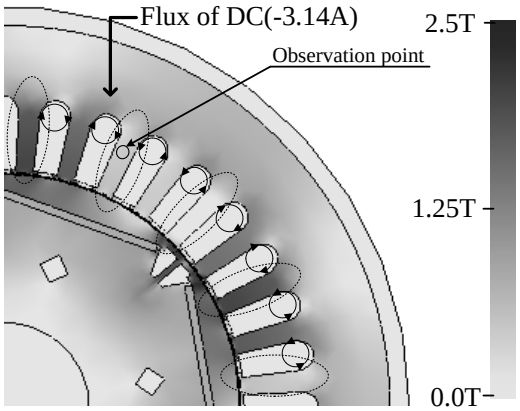

(b) With DC current.

Fig. 16. Magnetic flux density distribution.

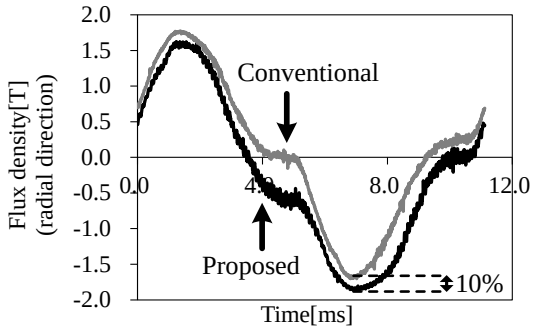

Fig. 17. Comparison of flux density.

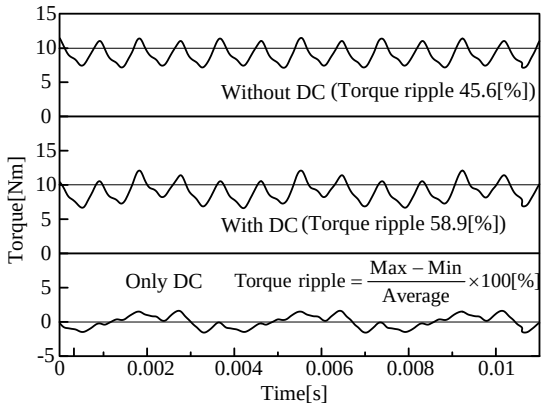

Fig. 18. Simulated torque waveforms.

approximately half of that of the conventional circuit.

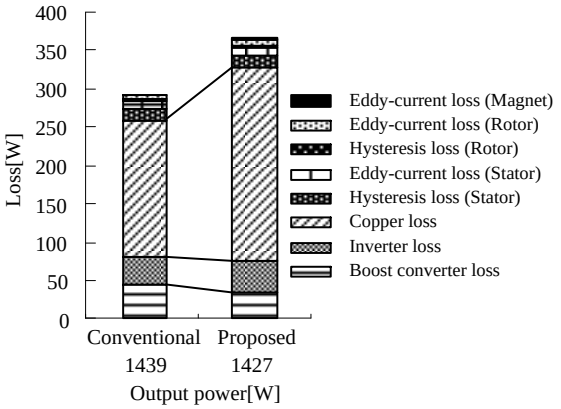

Fig. 19. Total loss analysis from simulation.

However, the copper loss of the motor is increased in the proposed circuit. In general, since the copper loss is proportional to the square of the motor current, DC component in the motor current degrades the efficiency. On the other hand, the iron loss remains unchanged provided that the magnetic flux saturation does not occur under this condition.

It should be noted that the analysis on the motor loss did not considered about the effect of the switching frequency component of the inverter output voltage.

VII. Conclusion

A novel two-stage DC/AC power converter connected to the neutral point of a motor was proposed. The proposed circuit can reduce the volume of the boost-up reactor and switching losses in the boost converter. Loss analysis confirmed a 1.7% increase in efficiency of the boost converter using the proposed circuit compared with that for a conventional circuit. The basic operation of the proposed circuit was confirmed by experimental results.

Six-step operation was applied to the proposed converter with feed forward control to compensate the fluctuation at the motor neutral point voltage. The experimental results confirmed that the proposed control method could suppress the input current distortion, reducing it to 1/8 of its original value.

In addition, the influence of imposed DC current was analyzed by a 2D FEM simulation for a 1.5 kW IPM motor. Analysis showed that the torque ripple was increased by 10% and the copper loss was increased by 30%. However, the increase of iron loss caused by the zero-phase current was very low. It should be noted that the torque ripple resulting from the third harmonic component could be compensated by feed forward control.

A trade off relationship between the converter and motor losses has been demonstrated in this paper. Future work will focus on the design structure of the motor in order to minimize the losses in the proposed circuit.

References

[1] Y.Tsuruta, and A.Kawamura, “Proposal of 98.5% High Efficiency Chopper Circuit QRAS for the Electric Vehicle

and the Verification," *Trans. IEEJ*, Vol.125, No.11, pp.977-987, 2005.

[2] D.Hirschmann, D.Tissen, S.Schroder, and R.W.De Doncker, "Reliability Prediction for Inverters in Hybrid Electrical Vehicles", *IEEE Transactions on Power Electronics*, pp. 2511-2517, Vol. 22, Issue.6, November 2007.

[3] Z.Du, B.Ozpineci L.M.Tolbert, and J.N.Chiasson, "DC–AC Cascaded H-Bridge Multilevel Boost Inverter With No Inductors for Electric/Hybrid Electric Vehicle Applications", *IEEE Transactions on Industry Applications*, pp. 963-970, Vol. 45, Issue.3, May/June 2009.

[4] M.Yamamoto, S.Sato, E.Hiraki, and M.Nakaoka, "New Space Vector Modulated 3-Level 3-Phase Voltage-Source Soft-Switching Inverter with Two Active Resonant DC Link Snubbers," *Trans. IEEJ*, Vol.123-D, No.12, pp.1397-1405, 2003.

[5] S.Inasaka, A.Kawamura, Y.Tsuruta "Research for High Efficient Electrical Power Management apply Bilateral Chopper for Electric Vehicle," *JIASC IEEJ*, pp.I-667-I-670, 2009.

[6] S.Nagai, S.Sato, M.Yamamoto, E.Hiraki, M.Nakaoka "Effective Improvement of DC Busline Voltage Utilization Factor in Two Switch-Auxiliary Quasi-Resonant DC Link Snubber Assisted Three Phase Voltage Source Type Soft-Switching PWM Inverter," *IEEJ Trans*. Vol.123-D, No.6, pp.710-716, 2003.

[7] L.Zhu, "A Novel Soft-Commutating Isolated Boost Full-Bridge ZVS-PWM DC–DC Converter for Bidirectional High Power Applications", *IEEE Transactions on Power Electronics*, pp. 422-429, Vol. 21, Issue.2, March 2006.

[8] Y.Zhang, and P.C.Sen, "A New Soft-Switching Technique for Buck, Boost, and Buck-Boost Converters", *IEEE Transactions on Industry Applications*, pp. 1775-1782, Vol. 39, Issue.6, November/December 2003.

[9] J.Itoh, and S.Ishii, "A Novel Single-phase High Power Factor Converter with Load Neutral Point Applied to PM Motor Drive," *Trans. IEEJ*, Vol.121-D, No.2, pp.219-224, 2001.

[10] K.Moriya, H.Nakai, Y.Inaguma and S.Sasaki "A DC/DC Converter Using Motor Neutral Point and its Control Method," *Annual meeting of IEEJ*, Vol.4, pp.119-120, 2004.

[11] T. Katagiri and J.Itoh: "PM motor driving with a boost type DC/AC conversion circuit using motor neutral point," *Annual meeting of IEEJ*, pp.142-143, 2007.

[12] S.Miaosen, S.Hodek, and F.Z.Peng, "Control of the Z-Source Inverter for FCHEV with the Battery Connected to the Motor Neutral Point", *IEEE Power Electronics Specialists Conference*, pp. 1485-1490, 2007

[13] Goh Teck Chiang and Jun-ichi Itoh, "DC/DC Boost Converter Functionality in a Three-Phase Indirect Matrix Converter", *IEEE Transactions on Power Electronics*, pp. 1559-1607, Vol. 26, Issue. 5, May 2011

[14] J.Itoh, J.Toyosaki, and H.Ohsawa, "High performance V/f control method for PM Motor," *Trans. IEEJ*, Vol.122-D,No.3 No.2 pp.253-259, 2002.

[15] J.Itoh, and N.Ohtani, "Square Wave Operation for a Single-phase PFC Three-phase Motor Drive System without a Reactor", *IEEE Transactions on Industry Applications*, pp. 805-811, Vol. 47, Issue.2, March-April 2011.

[16] H.Plesko, J.Biela, J.Luomi, and J.W.Kolar, "Novel Concepts for Integrating the Electric Drive and Auxiliary DC-DC Converter for Hybrid Vehicles", *IEEE Transactions on Power Electronics*, pp. 3025-3034, Vol. 23, Issue. 6, Nov. 2008.

Jun-Ichi Itoh (M'01) was born in Tokyo, Japan, in 1972. He received the M.S. and Ph.D. degrees in electrical and electronic systems engineering from Nagaoka University of Technology, Niigata, Japan, in 1996, 2000, respectively. From 1996 to 2004, he was with Fuji Electric Corporate Research and Development, Ltd., Tokyo, Japan. Since 2004, he has been with Nagaoka University of Technology, Niigata, Japan as Associate Professor. His research interests are matrix converters, dc/dc converters, power factor correction techniques and motor drives. Dr. Itoh received the IEEJ Academic Promotion Award (IEEJ Technical Development Award) in 2007. He is a member of the Institute of Electrical Engineers of Japan.

Ikarashi Daisuke (M'09) was born in Niigata, Japan, in 1986. He received the B.S. and M.S. degrees in electrical, electronics and information engineering from Nagaoka University of Technology, Nagaoka, Japan, in 2009 and 2011 respectively. Since 2011, he has been an employee of Hitachi research Laboratory, Hitachi, Ltd. He is the member of IEEJ and IEEE. His research interests include DC/AC converters.